

Stimulated Electromagnetic Emission near Electron Cyclotron Harmonics in the Ionosphere

T. B. Leyser, B. Thidé, H. Derblom, Å. Hedberg, and B. Lundborg
Swedish Institute of Space Physics, Uppsala Division, S-755 91 Uppsala, Sweden

P. Stubbe and H. Kopka

Max-Planck-Institut für Aeronomie, D-3411 Katlenburg-Lindau, Federal Republic of Germany
 (Received 20 March 1989)

Observations of electromagnetic emission stimulated by a high-frequency radio wave injected into the ionosphere from a ground-based powerful transmitter operated near harmonics of the ionospheric electron cyclotron frequency are reported. Significant changes in the spectrum of the stimulated electromagnetic radiation were obtained as the injected frequency was varied in small steps around these harmonics. The experimental results are attributed to nonlinear wave interactions involving electrostatic wave modes perpendicular to the local geomagnetic field.

PACS numbers: 52.35.Mw, 52.25.Sw, 94.20.Bb

A powerful high-frequency (hf) electromagnetic (em) wave in the ordinary mode, launched from the ground into the ionosphere, stimulates secondary em radiation in the sidebands of the reflected primary wave.¹⁻⁵ The spectra of these emissions depend on the ionospheric conditions as well as the frequency of the primary hf (pump) wave, f_0 , but exhibit in the general case a clear asymmetry as expected for parametric three-wave decay processes. If, however, f_0 is near a harmonic of the electron cyclotron frequency, f_{ce} , in the F region of the ionosphere, the spectral structure of the stimulated electromagnetic emission (SEE) is different and strongly dependent on f_0 as described in this Letter.

We present experimental results from the ionospheric modification facility Heating near Tromsø, Norway, obtained by varying the pump frequency in steps of 20 kHz between 5.343 and 5.483 MHz, which is near $4f_{ce}$. The pump wave was transmitted continuously for a few minutes on each frequency and the observed SEE spectra, as they appear a few seconds after the onset of the pump, persisted throughout this period. The effective radiated power of the vertically launched pump wave was 250 MW. The corresponding energy flux at 200-km altitude is approximately 0.5 mW/m², neglecting ionospheric absorption. The angle between the geomagnetic field and the downward vertical is approximately 13°.

Figures 1(a)-1(c) display three 200-kHz-wide spectra around the pump frequencies of 5.443, 5.403, and 5.383 MHz, respectively. In Fig. 1(a) two distinct features, the "downshifted maximum" (DM) and "broad upshifted maximum" (BUM), can be seen at $\Delta f_{DM} \approx -9$ kHz and $\Delta f_{BUM} \approx +35$ kHz, respectively. The DM feature, which is commonly observed for a wide range of pump frequencies,³ is absent in Fig. 1(b) and $\Delta f_{BUM} \approx +15$ kHz, whereas in Fig. 1(c) $\Delta f_{DM} \approx -9$ kHz and the BUM is absent. The strong spectral dependence on f_0 is typical and systematic and has been observed in several experiments with $f_0 \approx nf_{ce}$, $n=3,4,5$. As seen from

Figs. 1(a) and 1(b), Δf_{BUM} also depends strongly on f_0 . This dependency is summarized in Fig. 2.

We suggest that the pump excites upper hybrid waves through linear conversion facilitated by pump-induced geomagnetic field-aligned density striations,⁶⁻⁸ that are commonly detected during ionospheric modification experiments at Tromsø.⁹ These striations have a growth time of a few seconds, consistent with the rise time of the BUM and DM features. Also, it has been observed² that the SEE are strong whenever radar backscatter from striations are strong.

In order to study possible wave interactions involving upper hybrid waves, the general dispersion equation of linear waves in a homogeneous, magnetized plasma was solved numerically by using a kinetic-theory computer code.¹⁰⁻¹² Although density striations are present and may have a significant propagational effect on the waves,^{13,14} the plasma is assumed to be locally homogeneous so that our numerical model gives adequate information on the dispersion properties of the waves. Figure 3 displays the dispersion curves obtained for the upper hybrid (curves 1 and 3) and electron Bernstein modes (curves 2 and 4) for two choices of upper hybrid frequencies $f_{uh} = (f_{pe}^2 + f_{ce}^2)^{1/2}$ near $4f_{ce}$, corresponding to two different altitudes in the ionosphere; f_{pe} is the electron plasma frequency. Curves 1 and 2 are for $f_{uh}/f_{ce} = 3.80$. Curves 3 and 4 are for $f_{uh}/f_{ce} = 3.95$. For $f_0 < 4f_{ce}$, say $f_0 \approx 3.8f_{ce}$, there is a range of the perpendicular wave-vector component in which the perpendicular group velocity of the electrostatic waves is almost zero. The waves will therefore stay inside the field-aligned striations for a relatively long time and are thus susceptible to the largest enhancement by the hf wave. For $f_0 = 4f_{ce}$, resonant enhancement is weak because of strong cyclotron damping.^{15,16} For $f_0 > 4f_{ce}$, both the electron Bernstein mode for a wide range of electron plasma frequencies and the upper hybrid mode can be resonantly enhanced by the hf wave.

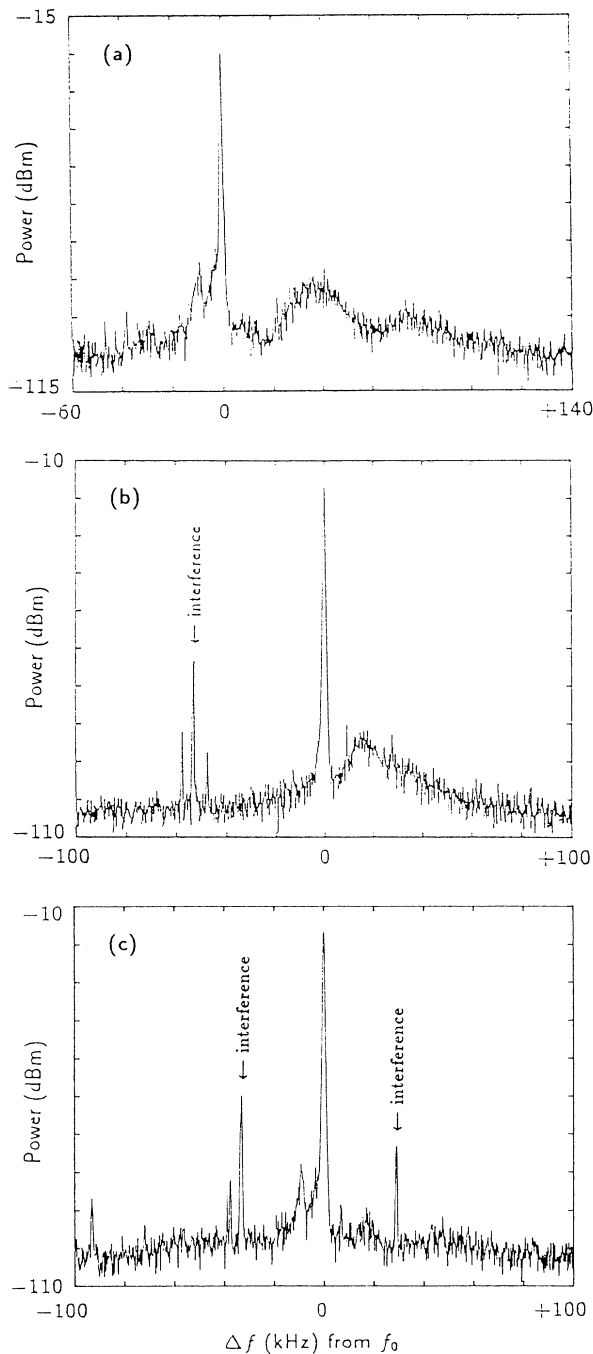


FIG. 1. Spectra of stimulated em emission for (a) $f_0 = 5.443$ MHz, (b) 5.403 MHz, and (c) 5.383 MHz. The spectra were recorded at Tromsø on 12 May 1988. The narrow features at $\approx -47, -53,$ and -57 kHz relative to f_0 in (b), and the corresponding features in (c), are interferences from nearby hf transmitters.

The enhanced upper hybrid wave (f_1, \mathbf{k}_1) decays into an em wave (f_2, \mathbf{k}_2) in the ordinary mode and a lower hybrid wave (f_3, \mathbf{k}_3). The em wave, with a frequency

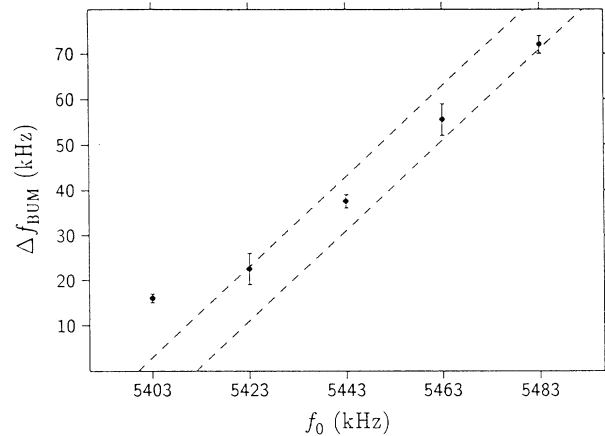


FIG. 2. The offset of the BUM feature, $\Delta f_{\text{BUM}} = f_{\text{BUM}} - f_0$ (in kHz) vs f_0 near $4f_{ce}$. The two dashed lines are given by $f_{\text{BUM}} = 2f_0 - 4f_{ce}$, where $f_{ce} = 1.350$ and 1.353 MHz, respectively.

$f_2 \approx f_1 - f_3 > f_{pe}$, can escape from the ionosphere and be detected on the ground. It must be in the ordinary mode since the extraordinary mode is evanescent at the upper hybrid resonance, where $f_{1,2} \approx f_{\text{uh}}$. This parametric instability has been suggested to explain narrow-band radio-wave emission in the magnetosphere.^{17,18} Taking \mathbf{k}_2 parallel to the geomagnetic field and applying formula (42) of Ref. 18 to conditions in the F region yields a low instability threshold (< 1 V/m). We suggest that this parametric process can explain hitherto unexplained properties of the commonly observed DM feature in the SEE spectra. The growth rate for the lower hybrid wave is highest (and the threshold lowest) at the lower hybrid frequency, which is approximately 8 kHz in the F region above Tromsø. This is consistent with the steep edge of the DM at 8 kHz below the pump [Figs. 1(a) and 1(c)]. The parametric interaction suggested here is also consistent with the lack of correlation between the DM feature and measurements of incoherent scatter using the EISCAT-UHF facility,¹⁹ since the radar line of sight was approximately parallel to the geomagnetic field prohibiting the detection of electrostatic waves having wave vectors perpendicular to the geomagnetic field. Further, just at the electron cyclotron harmonics the upper hybrid waves are strongly damped, which is consistent with the disappearance of the DM feature for certain hf frequencies. Assuming that $f_0 = 5.403$ MHz, for which the DM did not develop [Fig. 1(b)], is exactly at the fourth harmonic, we obtain $f_{ce} = 1.35$ MHz. For the experiments at the third and fifth harmonics we obtain $f_{ce} = 1.36$ and 1.35 MHz, respectively. These values are in good agreement with models of the geomagnetic field in the F region above Tromsø.

The data points in Fig. 2 closely follow the relation $f_{\text{BUM}} = 2f_0 - 4f_{ce}$, or $2f_0 = f_{\text{BUM}} + 4f_{ce}$, where f_{BUM} is the frequency of the BUM. This empirical relation sug-

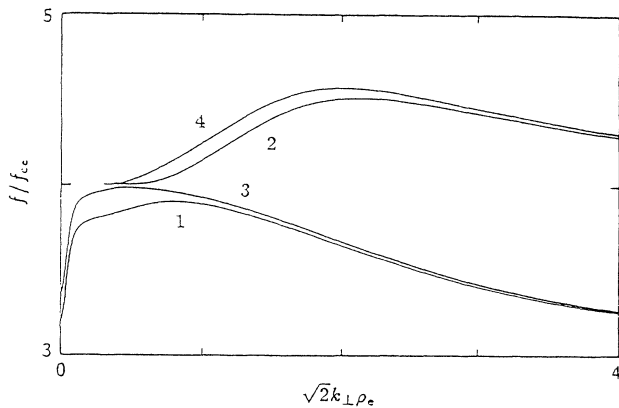


FIG. 3. Dispersion curves for the upper hybrid mode (curves 1 and 3) and the electron Bernstein mode (curves 2 and 4) for $k_{\parallel} = 10^{-4} \text{ m}^{-1}$, $f_{ce} = 1.350 \text{ MHz}$, $T_e = 1600 \text{ K}$, and $T_i = 800 \text{ K}$ for the O^+ ions; ρ_e is the thermal electron gyroradius. Curves 1 and 2 are for $f_{uh}/f_{ce} = 3.80$ and curves 3 and 4 for $f_{uh}/f_{ce} = 3.95$.

gests that the BUM feature is generated through a four-wave interaction, involving two pump photons or upper hybrid plasmons, a decay mode at $4f_{ce}$, and the stimulated radiation at f_{BUM} . Assuming that the BUM feature is generated exactly at nf_{ce} , the spectral width can be used to estimate the altitude range in which the emissions are generated. With a spectral width of approximately 20 kHz [Fig. 1(a)] at the fourth cyclotron harmonic the range in electron cyclotron frequency is 5 kHz. This corresponds to an altitude range of approximately 5 km.

In conclusion, our experiments suggest that nonlinear interactions between wave modes perpendicular to the geomagnetic field stimulate em emission during high-frequency ionospheric modification experiments. The experiments reveal a high sensitivity of some spectral features of the SEE on the pump frequency. These significant changes in the stimulated radiation spectrum are associated with the pump frequency being close to, or at, harmonics of the electron cyclotron frequency in the ionospheric *F* region. We suggest that the ordinary mode pump wave excites upper hybrid waves through linear conversion facilitated by the presence of pump-induced density striations in the upper hybrid resonance

region. The stimulated em radiation can be used to determine the magnitude of the geomagnetic field where the upper hybrid frequency matches electron cyclotron harmonics in the ionosphere.

The Swedish authors gratefully acknowledge the financial support from the Swedish Natural Science Research Council (NFR) and the logistic support from the Auroral Observatory, Tromsø. The Heating project has been financially supported by the Deutsche Forschungsgemeinschaft (DFG).

¹B. Thidé, H. Kopka, and P. Stubbe, *Phys. Rev. Lett.* **49**, 1561 (1982).

²B. Thidé, H. Derblom, Å. Hedberg, H. Kopka, and P. Stubbe, *Radio Sci.* **18**, 851 (1983).

³P. Stubbe, H. Kopka, B. Thidé, and H. Derblom, *J. Geophys. Res.* **89**, 7523 (1984).

⁴G. N. Boiko, L. M. Erukhimov, V. A. Zyuzin, G. P. Komrakov, S. A. Metelev, N. A. Mityakov, V. A. Nikonov, V. A. Ryzhov, Yu. V. Tokarev, and V. L. Frolov, *Radiophys. Quantum Electron.* **28**, 259 (1985).

⁵J. A. Fejer, C. A. Gonzales, H. M. Ierick, M. P. Sulzer, C. A. Tepley, L. M. Duncan, F. T. Djuth, S. Ganguly, and W. E. Gordon, *J. Atmos. Terr. Phys.* **47**, 1165 (1985).

⁶V. V. Vas'kov and A. V. Gurevich, *Zh. Eksp. Teor. Fiz.* **73**, 923 (1977) [*Sov. Phys. JETP* **46**, 487 (1977)].

⁷A. C. Das and J. A. Fejer, *J. Geophys. Res.* **84**, 6701 (1979).

⁸B. Inhester, A. C. Das, and J. A. Fejer, *J. Geophys. Res.* **86**, 9101 (1981).

⁹Å. Hedberg, H. Derblom, B. Thidé, H. Kopka, and P. Stubbe, *Radio Sci.* **18**, 840 (1983).

¹⁰K. Rönnmark, Swedish Institute of Space Physics, KGI Report No. 179, 1982 (unpublished).

¹¹K. Rönnmark, *Plasma Phys.* **25**, 699 (1983).

¹²M. André, *J. Plasma Phys.* **33**, 1 (1985).

¹³J. R. McAfee, *J. Geophys. Res.* **73**, 5577 (1968).

¹⁴D. B. Muldrew, *J. Geophys. Res.* **83**, 2552 (1978).

¹⁵G. Bekefi, *Radiation Processes in Plasmas* (Wiley, New York, 1966), pp. 234–238.

¹⁶I. P. Shkarofsky, *Phys. Fluids* **9**, 570 (1966).

¹⁷D. D. Barbosa, *Rev. Geophys. Space Phys.* **20**, 316 (1982).

¹⁸G. Murtaza and P. K. Shukla, *J. Plasma Phys.* **31**, 423 (1984).

¹⁹J. A. Nordling, Å. Hedberg, G. Wannberg, T. B. Leyser, H. Derblom, H. J. Opgenoorth, H. Kopka, H. Kohl, P. Stubbe, M. T. Rietveld, and C. LaHoz, *Radio Sci.* **23**, 809 (1988).